

# Decreased polarity and increased random motility in PtK1 epithelial cells correlate with inhibition of endosomal recycling

Natalie L. Prigozhina<sup>1</sup> and Clare M. Waterman-Storer<sup>2</sup>

<sup>1</sup>The Burnham Institute, 10901 N. Torrey Pines Road, Room 7108, La Jolla, CA 92037, USA

<sup>2</sup>The Scripps Research Institute, Department of Cell Biology, CB163, 10550 N. Torrey Pines Road, La Jolla, CA 92037, USA

Authors for correspondence (e-mail: nataliep@burnham.org; waterman@scripps.edu)

Accepted 24 May 2006

*Journal of Cell Science* 119, 3571-3582 Published by The Company of Biologists 2006  
doi:10.1242/jcs.03066

## Summary

Locomoting cells exhibit a constant retrograde flow of plasma membrane proteins from the leading edge towards the cell center, which, when coupled to substrate adhesion, may drive forward cell movement. Here, we aimed to test the hypothesis that, in epithelial cells, these plasma membrane components are delivered via a polarized endo/exocytotic cycle, and that their correct recycling is required for normal migration. To this end, we expressed in PtK1 cells cDNA constructs encoding GDP-restricted (S25N) and GTP-restricted (Q70L) mutants of Rab11b, a small GTPase that has been implicated in the late stage of recycling, where membrane components from the endosomal recycling compartment are transported back to the plasma membrane. Surprisingly, we found that transient expression of the Rab11b mutants in randomly

migrating PtK1 cells in small cell islands caused altered cell morphology and actually increased the velocity of cell locomotion. Stable expression of either mutant protein also did not decrease cell migration velocity, but instead affected the directionality of migration in monolayer wound healing assays. We have also tested the effects of other Rab proteins, implicated in endocytic recycling, and discovered a clear correlation between the degree of recycling inhibition and the increase in non-directional cell motility.

Supplementary material available online at  
<http://jcs.biologists.org/cgi/content/full/119/17/3571/DC1>

Key words: Cell motility, Recycling, Directional migration, Membrane traffic, Epithelial cells, Cell morphology

## Introduction

Migrating cells exhibit a constant retrograde flow of plasma membrane (PM) proteins from the leading edge lamellipodium backwards towards the cell center. It has been suggested that this flow, when coupled to substrate adhesion, may drive forward cell movement (Heath and Holifield, 1991; Mitchison and Cramer, 1996; Ridley et al., 2003). However, the intracellular source of these PM components and whether their continuous delivery to the leading edge is needed for cell motility is largely unknown. Two possible mechanisms for supplying these materials to the leading edge of migrating cells have been proposed. One suggests that the components may be delivered via a polarized endo/exocytotic cycle (i.e. recycling) (Bretscher, 1992; Bretscher, 1984; Bretscher and Aguado-Velasco, 1998b; Hopkins et al., 1994), and the other suggests that they maybe newly synthesized and delivered to the leading edge via the anterograde secretion pathway (Bergmann et al., 1983; Prigozhina and Waterman-Storer, 2004).

In our previous work (Prigozhina and Waterman-Storer, 2004) we showed by inhibiting the budding of membrane cargo from the trans-Golgi network using a dominant negative mutant of protein kinase D that, in fibroblasts, directional locomotion depends on the anterograde secretion pathway. However, when we similarly inhibited the anterograde secretion pathway in epithelial PtK1 cells, their motility was unaffected (our unpublished data). Therefore, it is possible that

migrating fibroblasts and epithelial cells may preferentially rely on different membrane trafficking pathways to supply PM components for retrograde flow and leading edge advancement.

Here, we aim to test the hypothesis that epithelial cells may utilize the polarized endosomal recycling pathway to support their migration. The endosomal recycling pathway (Fig. 1) is comprised of several types of endosomes, including early/sorting endosomes (EE), and the endocytic recycling compartment (ERC), which is generally located at the cell center, near the Golgi apparatus (GA) (reviewed in Mukherjee et al., 1997). Many regulatory components of the endosomal pathway have been identified, including a number of Rabs, small GTPases that regulate distinct steps in the intracellular membrane pathways (Maxfield and McGraw, 2004; Mohrmann and van der Sluijs, 1999; Rodman and Wandinger-Ness, 2000; Sonnichsen et al., 2000; Zerial and McBride, 2001). Transferrin, a commonly used marker of the endocytic recycling pathway, binds to cell surface receptors that are internalized via clathrin-coated vesicles in a Rab5-dependent manner to form the EE (Bucci et al., 1992). Most of the transferrin is recycled back to the cell surface via the slow recycling pathway through the ERC in a process that requires Rab11, and some transferrin is recycled directly from the EE in Rab4-dependent fast recycling (Bretscher, 1992; Chavrier et al., 1997; Daro et al., 1996; Hopkins et al., 1994; Mohrmann et al., 2002; Trischler et al., 1999; Yamashiro et al., 1984).

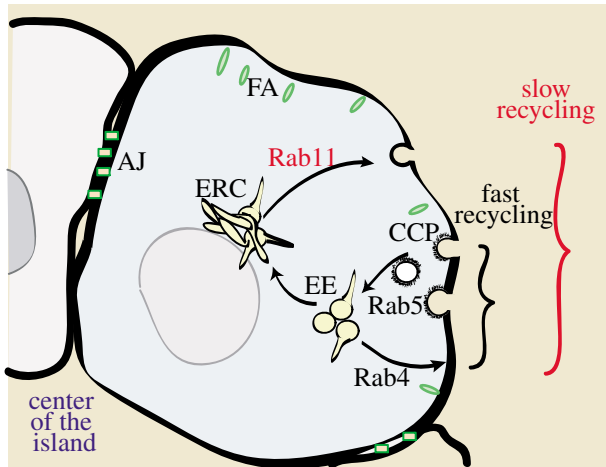


**Fig. 1.** Recycling in a cell at the edge of epithelial island. AJ, adherens junctions; CCP, clathrin-coated pits; EE, early/sorting endosomes; ERC, endosomal recycling compartment; FA, focal adhesions; LE, late endosomes. Relevant Rab players are indicated (Rab4, Rab5 and Rab11).

Several studies support a specific role for endosomal recycling in cell migration. For example, it has been shown that in migrating neutrophils an integrin (molecule that mediates adhesion and migration) recycles from the cell rear to the lamellipodium at the cell front through polarized endosomal recycling (Pierini et al., 2000). In KB cells, surface ruffles may arise by exocytosis of internal membrane from the endosomal cycle (Bretscher and Aguado-Velasco, 1998a). There is some evidence that inhibition of the recycling pathway by expressing a dominant negative mutant of Rab11 or C-terminal fragment of its effector rabphilin11 may cause decreased motility in MDCK and HeLa cells, although this effect has not been very well characterized (Mammoto et al., 1999). Rab5 expression was shown to induce lamellipodia formation and cell migration (Spaargaren and Bos, 1999). Finally, numerous studies (reviewed in Sabe, 2003) established the connection between cell migration and a small GTPase ARF6, which is also involved in regulating recycling.

To investigate the role of recycling in the motility of epithelial cells, we here sought to inhibit Rab11-dependent slow recycling from the ERC to the PM. There are two closely related homologues of Rab11, both ubiquitously expressed and localized to distinct cellular compartments (Lapierre et al., 2003). The better studied Rab11a (Goldenring et al., 1996) is involved in TGN trafficking (Chen et al., 1998; Chen and Wandinger-Ness, 2001; Urbe et al., 1993; Wilcke et al., 2000) as well as recycling through the ERC (Green et al., 1997; Ren et al., 1998; Ullrich et al., 1996; Volpicelli et al., 2002). Rab11b function has been implicated in recycling from ERC (Schlierf et al., 2000). In this study we used GDP and/or GTP-restricted mutants of Rab11b and other Rab proteins (Rab11a and Rab4a) to perturb the intracellular recycling machinery and investigate its role in epithelial cell motility. We found that inhibiting recycling by expressing these mutants in PtK1 kidney epithelial cells leads to decreased cell area and abnormal morphology. Surprisingly, contrary to our expectations, lamellipodial activity and migration of these cells increased, rather than decreased. The directionality of migration,

however, was markedly diminished. Thus, we propose a modification of the original hypothesis that endosomal recycling is required for cell migration. Instead, it appears that normal recycling may regulate cell morphology and polarity and, when disrupted, increases disorganized motility.

## Results

### Localization of Rab11b in PtK1 cells

We aimed to test for the requirement of the slow endosomal recycling pathway in PtK1 epithelial cell motility by disrupting the activity of Rab11b. To perturb Rab11b, we expressed GFP-conjugated dominant-negative mutants (constitutively GDP-bound S25N and constitutively GTP bound Q70L) that are unable to carry out a normal GTP hydrolysis cycle (Lai et al., 1994; Schlierf et al., 2000). These mutants shall be referred to as  $\text{GFP}^{\text{Rab11b-GDP}}$  and  $\text{GFP}^{\text{Rab11b-GTP}}$ , respectively. First, we created PtK1 cell lines that stably express these mutants and examined the intracellular localization of the  $\text{GFP}^{\text{Rab11b}}$  proteins by live-cell imaging and/or indirect immunofluorescence. As can be seen from Fig. 2A,B,  $\text{GFP}^{\text{Rab11b-GDP}}$  was observed predominantly in fine tubules emanating from the perinuclear area, while  $\text{GFP}^{\text{Rab11b-GTP}}$  was also concentrated in the perinuclear region but the labeled structures appeared to be more vesiculated. Similar Rab11b-positive structures were also seen in live PtK1 cells that had been microinjected in their nuclei with appropriate plasmids to transiently express the same wild-type and mutant Rab11b proteins (data not shown). As can be seen in cells fixed and processed for immunofluorescence after microinjection of the  $\text{GFP}^{\text{Rab11b-GDP}}$  construct (Fig. 3D,E), the expressed  $\text{GFP}^{\text{Rab11b-GDP}}$  colocalized with the anti-Rab11 antibody, although the tubular structures observed in live cells were mostly lost during fixation. We also found that a portion of the overexpressed Rab11b mutants was localized to the cis/medial Golgi apparatus but not to the trans-Golgi Network (TGN), as confirmed by lectin, anti-mannosidase II and anti-TGN38 labeling (data not shown).

To determine whether  $\text{GFP}^{\text{Rab11b}}$ -labeled structures were indeed relevant to endosomal trafficking, we tested whether they colocalized with fluorescently labeled transferrin, a well-characterized recycling marker, during its route through the endosomal recycling pathway. To this end, we performed a pulse-chase labeling experiment. Cells stably expressing wild-type, and GTP and GDP mutant Rab11b constructs were incubated on ice in the presence of fluorescently labeled transferrin. This allowed transferrin to bind to the cell surface receptors but did not result in its internalization. There was no statistically significant difference in transferrin binding between control PtK1 cells and the stable cell lines expressing Rab11b mutants (data not shown). Subsequently, the cells were transferred to transferrin-free media, quickly warmed up to 37°C to induce synchronous transferrin internalization, and were immediately observed by high-resolution live-cell microscopy. For both GDP- and GTP-bound  $\text{GFP}^{\text{Rab11b}}$ , this revealed that fluorescent transferrin first appeared in GFP-positive tubulo-vesicular compartments in about 5 minutes after internalization (Fig. 2D,E and supplementary material Movies 2a and 3a). The colocalization typically continued for about 10 minutes and then disappeared (Fig. 2G,H and supplementary material Movies 2b and 3b). Note how, in the case of  $\text{GFP}^{\text{Rab11b-GDP}}$ , at 5 minutes after internalization both

$GFP^{Rab11b}$ -GDP and transferrin colocalized in tubulo-vesicular structures, but later transferrin was found predominantly in vesicles while  $GFP^{Rab11b}$ -GDP localization remained tubulo-vesicular. The transient nature of colocalization between Rab11b and transferrin argued against complete transferrin arrest in the Rab11b-positive compartment and suggested that the recycling process may be slowed but not completely inhibited, possibly with transferrin being redirected to the peripheral structures rather than going through the central ERC.

To determine the degree of colocalization between  $GFP^{Rab11b}$  proteins and labeled transferrin during steady-state recycling, we incubated cells that were transiently expressing Rab11b proteins with labeled transferrin at 37°C for 45 minutes. As can be seen in cells expressing the  $GFP^{Rab11b}$ -GDP construct (Fig. 3), colocalization between  $GFP^{Rab11b}$ -GDP and the labeled transferrin could be observed in both the peripheral structures (Fig. 3A-C) and in the perinuclear ERC region (Fig. 3D-G). Similar results were obtained with the GTP-restricted Rab11b mutant (data not shown). Together, these results indicate that exogenously expressed  $GFP^{Rab11b}$  mutants faithfully localize to endosomal structures.

#### Transferrin recycling is inhibited in cells expressing $GFP^{Rab11b}$ -GDP

To find out if perturbing Rab11b function indeed caused defects in slow recycling from the ERC, we studied the effects of  $GFP^{Rab11b}$ -GDP expression on transferrin recycling. We

chose the GDP-restricted mutant because (1) similar morphological phenotypes were observed in cell expressing either GDP- or GTP-restricted Rab11b mutants (see below), (2) normal function of Rab proteins requires cycling between GTP and GDP forms, thus often rendering both GDP- and GTP-restricted mutants dominant negative, and (3) our results were in agreement with previous data (Schlierf et al., 2000).

To assure the specificity of human transferrin binding to and uptake by PtK1 cells, we incubated the cells with increasing concentrations of both Alexa568-transferrin and FITC-dextran either on ice, or under steady-state loading condition at 37°C. If human transferrin were internalized by non-specific mechanisms (i.e. bulk endocytosis), we would expect to see similar behavior between Alexa568-transferrin and FITC-dextran, a bulk endocytosis marker. By contrast, we found that, unlike FITC-dextran, both transferrin binding and steady-state loading were concentration-dependent and also much more effective than dextran (Fig. 4E). It is likely that, at the concentrations used, the bulk endocytosis visualized by FITC-dextran uptake was saturated, while receptor-mediated endocytosis of Alexa568-transferrin was not. Overall, this indicated that Alexa568-transferrin and FITC-dextran were internalized by different mechanisms, and that Alexa568-transferrin uptake was, therefore, specific.

To test whether  $GFP^{Rab11b}$ -GDP expression inhibited transferrin recycling, we injected the nuclei of PtK1 cells with plasmid encoding  $GFP^{Rab11b}$ -GDP, allowed 3.5-4 hours for expression of the construct and incubated the cells in serum free media for 1 hour. We then either let them

bind fluorescently labeled Alexa568-transferrin on ice, subsequently transferring them to 37°C for a 30 minute chase period in serum-containing media without labeled transferrin (Fig. 4A-D), or let them internalize transferrin at 37°C for a period of 45 minutes under serum-free conditions and then chasing similarly (Fig. 4F,G and all subsequent quantitative analysis). In both types of experiments we observed significant amounts of transferrin retained in the  $GFP^{Rab11b}$ -GDP-expressing cells after the chase period compared with the neighboring control cells (Fig. 4D and images not shown). Next, we quantified the effects of  $GFP^{Rab11b}$ -GDP expression on recycling after steady-state uptake. The amount of internalized transferrin (as judged by the total Alexa 568 fluorescence inside the cells) was

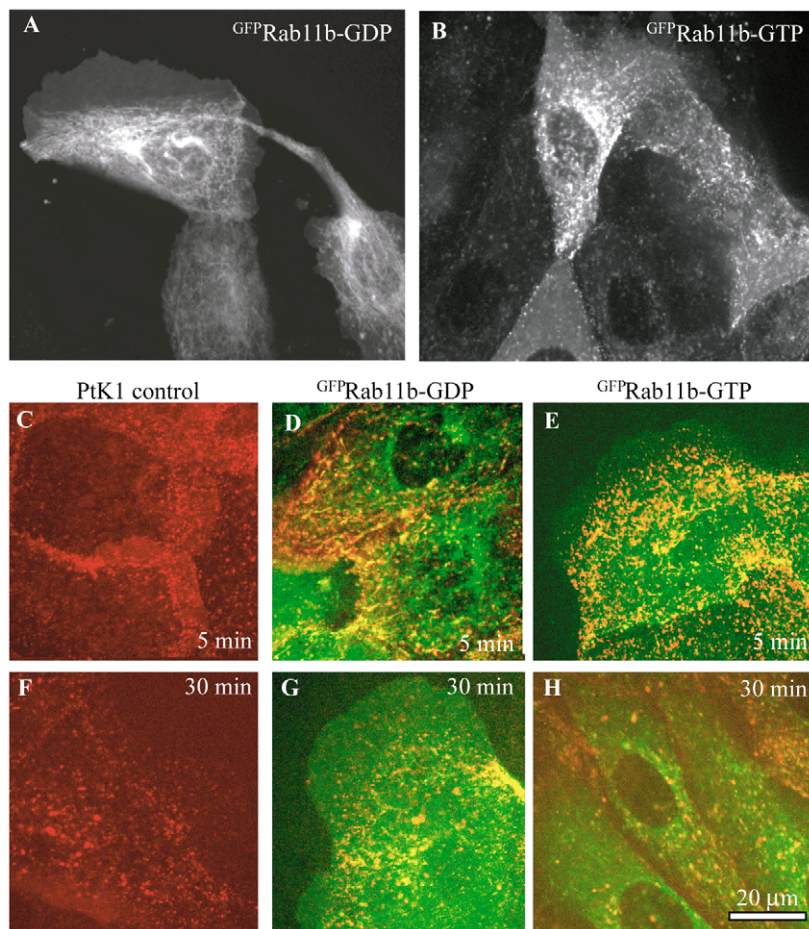


**Fig. 2.**  $GFP^{Rab11b}$  localization in stably expressing PtK1 cell lines. Confocal images of living PtK1 cells expressing  $GFP^{Rab11b}$ -GDP (A,D,G) and  $GFP^{Rab11b}$ -GTP (B,E,H) visualized by GFP fluorescence. Alexa-568-transferrin (red) in control cells (C,F) and in cells stably expressing the  $GFP^{Rab11b}$  mutants (D,E,G,H). Live cell images were taken approximately 5 minutes (C-E) or 30 minutes (F-H) after transferrin internalization was induced by a shift from 0°C to 37°C. Corresponding supplemental movies are available for control (supplementary material Movie 1a,b),  $GFP^{Rab11b}$ -GDP (supplementary material Movie 2a,b) and  $GFP^{Rab11b}$ -GTP (supplementary material Movie 3a,b) cells.

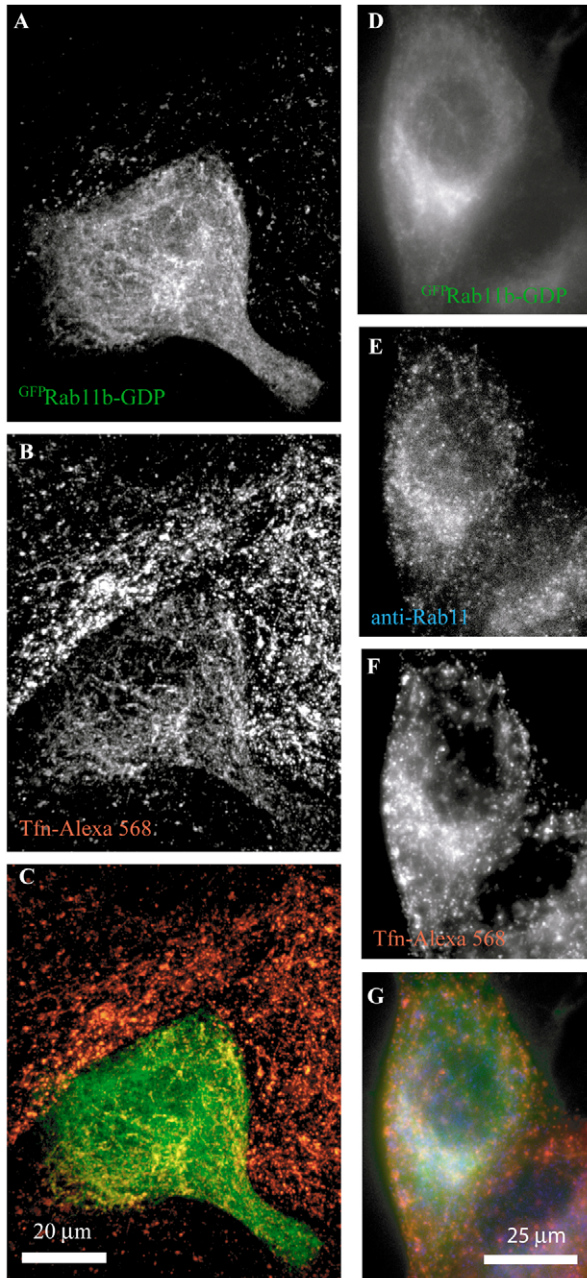


**Fig. 3.** Rab11b-GFP localization in transiently expressing cells. A live  $\text{GFP}^{\text{Rab11b-GDP}}$ -expressing cell showing partial colocalization of the  $\text{GFP}^{\text{Rab11b-GDP}}$  (A) with Alexa-568-transferrin internalized under steady-state conditions (B). (C)  $\text{GFP}^{\text{Rab11b-GDP}}$  (green), Alexa 568 transferrin (red). Colocalization (G, white) between  $\text{GFP}^{\text{Rab11b-GDP}}$  (D,G, green), antibodies against Rab11 (E,G, blue) and Alexa-568-transferrin (F,G, red).

similar or slightly higher in the  $\text{GFP}^{\text{Rab11b-GDP}}$ -expressing cells compared with the neighboring control cells (data not shown). This was to be expected since any problems in recycling would cause the cells to accumulate more marker during the 45 minutes of incubation. At the end of the chase period, the control cells had very little transferrin left in them, in stark contrast to the  $\text{GFP}^{\text{Rab11b-GDP}}$ -expressing cells,

which appeared much brighter and contained much more transferrin than their control neighbors. The percent transferrin recycling in  $\text{GFP}^{\text{Rab11b-GDP}}$ -expressing cells amounted to only  $29 \pm 11\%$ , while control cells recycled transferrin much more efficiently ( $79 \pm 3.1\%$ ) (Fig. 4F, Table 1). When we directly compared neighboring control and mutant cells from the same coverslips, we found that the recycling efficiency in  $\text{GFP}^{\text{Rab11b-GDP}}$ -expressing cells was only 35% compared with that in the control cells (Fig. 4G, Table 1). Thus, the rate of recycling in cells transiently expressing  $\text{GFP}^{\text{Rab11b-GDP}}$  was, indeed, diminished compared with the control cells.

Because of the high variability in expression, we were not able to do similar analysis in the cell line stably expressing  $\text{GFP}^{\text{Rab11b-GDP}}$ . However, as can be seen in Fig. 4H, cells expressing higher levels of  $\text{GFP}^{\text{Rab11b-GDP}}$  retained more fluorescently labeled transferrin after 1 hour of recycling than cells expressing lower levels of  $\text{GFP}^{\text{Rab11b-GDP}}$ . Thus, in both stable and transient expression systems,  $\text{GFP}^{\text{Rab11b-GDP}}$  expression correlated with a reduced ability to recycle transferrin.

#### PtK1 cells transiently expressing $\text{GFP}^{\text{Rab11b}}$ proteins move with increased velocities and exhibit abnormal morphology

In order to test the effects of transient expression of  $\text{GFP}^{\text{Rab11b}}$  mutants on cell morphology and migration, we microinjected the plasmids encoding these proteins into PtK1 nuclei and observed cell behavior after 4–5 hours of expression. For this approach we chose cells at the edges of small (4–6 cells) to medium (8–12 cells) sized epithelial cell clusters ('islands'). Control cell islands lacking exogenous protein expression were well spread and remained tightly associated with each other as they randomly migrated together as a unit in a more-or-less coordinated fashion (Fig. 5A,D, and supplementary material Movie 4). The cells in such islands typically had their lamellipodial activity polarized at the free edge, while the contacted edges remained relatively quiescent. By contrast, PtK1 cells transiently expressing  $\text{GFP}^{\text{Rab11b}}$  mutants exhibited altered morphologies (Fig. 5B,C). Specifically, expression of either mutant caused cells within islands to appear 'thicker' and be less spread compared with control cells. The mutant cells also changed direction more randomly, moved in a less coordinated fashion (Fig. 5E,F, and supplementary material Movies 5 and 6), and their protrusional activity was more dispersed over the cell periphery. Additionally,  $\text{GFP}^{\text{Rab11b-GDP}}$ -expressing cells often broke cell-cell contacts with their neighbors and sometimes exhibited long tails that failed to detach from the substrate and/or other cells (Fig. 5C). If most cells in an island were expressing the  $\text{GFP}^{\text{Rab11b-GDP}}$  (as in Fig. 5C), often the whole island scattered.

Next, we measured migration parameters of cells in islands from time-lapse image series. Unexpectedly, this revealed that cells expressing either  $\text{GFP}^{\text{Rab11b-GTP}}$  or  $\text{GFP}^{\text{Rab11b-GDP}}$  proteins migrated significantly faster than controls ( $0.78 \pm 0.08$   $\mu\text{m}/\text{minute}$  for both  $\text{GFP}^{\text{Rab11b-GDP}}$  and  $\text{GFP}^{\text{Rab11b-GTP}}$  compared to  $0.49 \pm 0.03$   $\mu\text{m}/\text{minute}$  for control cells).

#### PtK1 cells stably expressing Rab11b proteins lose their polarity and exhibit abnormal migratory behavior in wound healing assays

We used stable PtK1 cell lines expressing either GDP- or GTP-

restricted mutants of  $\text{GFP}^{\text{Rab11b}}$  to look at the effects of these proteins on directional migration in wound assays. For these assays, we allowed the cells to grow to confluency, scratched a wound in the cell layer using a micropipette tip, and monitored cell migration into the wound by time-lapse microscopy. Control cells that did not express exogenous proteins, migrated as a unified front and effectively healed the wound within 6 hours of observation (Fig. 6A,B,

supplementary material Movie 7). By contrast, the wound edge advancement of the cells expressing mutant  $\text{GFP}^{\text{Rab11b}}$  proteins was much more disorganized (Fig. 6D-E,G-H, supplementary material Movies 8 and 9). In about 6 hours, total translocation of the control wound edge amounted to  $125.3 \pm 70.8 \mu\text{m}$ , while the edges of wounds in monolayers of  $\text{GFP}^{\text{Rab11b-GDP}}$ - and  $\text{GFP}^{\text{Rab11b-GTP}}$ -expressing cells translocated only  $11.3 \pm 17.8 \mu\text{m}$  and  $14.5 \pm 46.1 \mu\text{m}$ ,

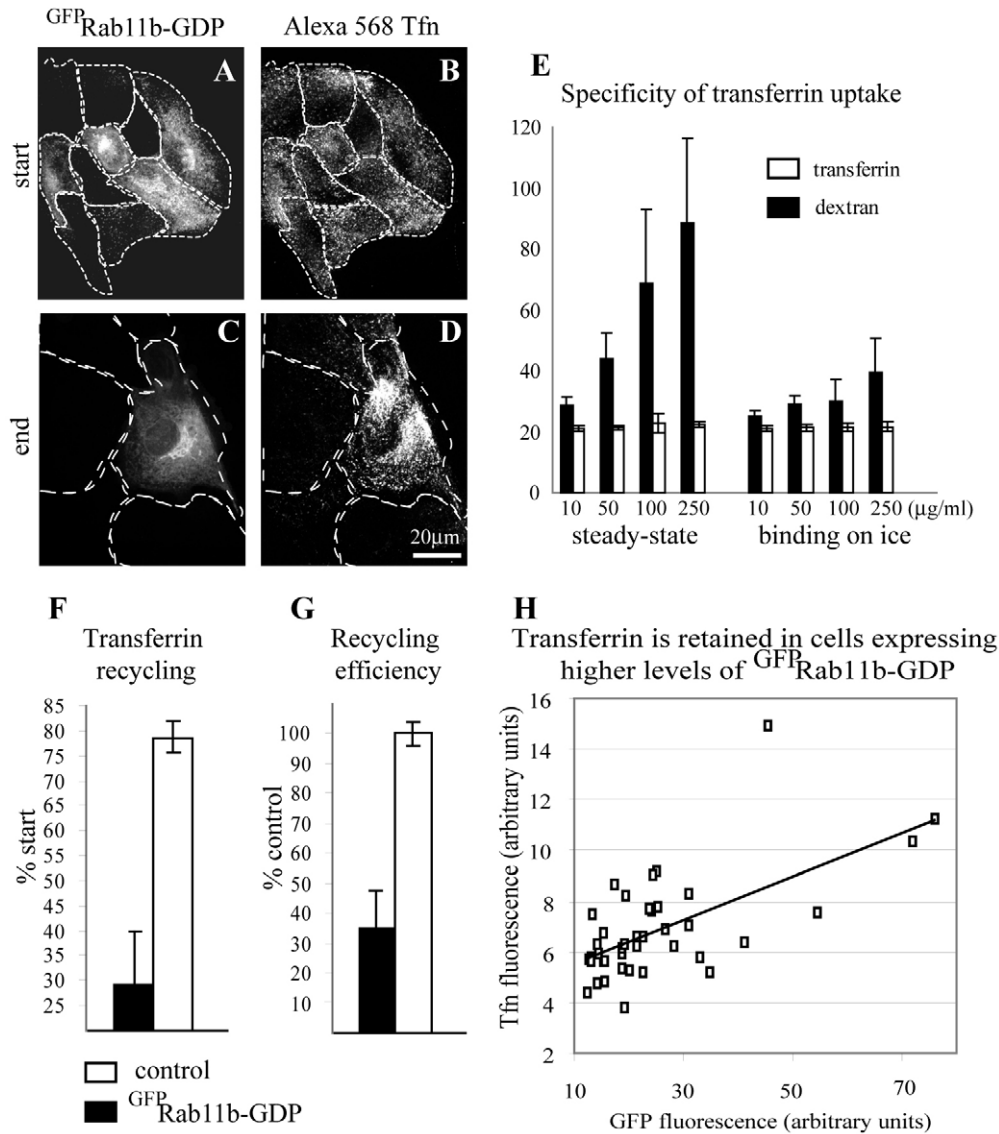


**Fig. 4.** Transferrin recycling is inhibited in cells expressing  $\text{GFP}^{\text{Rab11b}}$  mutants. (A,B) Binding (on ice) of Alexa-568-transferrin to control and to cells transiently expressing  $\text{GFP}^{\text{Rab11b-GDP}}$ . (C,D) Transferrin retained in the  $\text{GFP}^{\text{Rab11b-GDP}}$ -expressing cell after a 30 minute chase at  $37^\circ\text{C}$ . The outlines of individual cells in the island are indicated by dotted lines. (A,C)  $\text{GFP}^{\text{Rab11b-GDP}}$ -expressing cells identified by GFP fluorescence; (B,D) Alexa-568-transferrin. (E) An assay for specificity of transferrin binding and uptake by PtK1 cells. Cells were incubated with increasing concentrations (10, 50, 100 and 250  $\mu\text{g/ml}$  each) of fluorescently labeled Alexa568-transferrin and FITC-dextran either at  $37^\circ\text{C}$  or on ice. Each bar represents average fluorescence intensity of approximately 100 cells per condition. Each condition was assayed in three different wells, four fields of view per well and analyzed using Thora software. (F) Transferrin recycling in cells transiently expressing  $\text{GFP}^{\text{Rab11b-GDP}}$ , measured as fluorescent intensity of Alexa-568-transferrin retained inside the cells at the end of a 30-minute chase period, and expressed as a percentage of total transferrin bound at the beginning of experiment. (G) Recycling efficiency in cells transiently expressing  $\text{GFP}^{\text{Rab11b-GDP}}$ , expressed as a percentage of neighboring control cells values. All data are mean  $\pm$  s.e.m., calculated from at least three experiments, 20-40 cells per experiment. (H) Correlation between the  $\text{GFP}^{\text{Rab11b-GDP}}$  expression level in a stable  $\text{GFP}^{\text{Rab11b-GDP}}$  cell line and transferrin retained inside the cells after a 1 hour recycling period. Data for 40 cells from a representative experiment are shown.

**Table 1. Recycling and velocity values for cells transiently expressing various Rab mutants**

	Transferrin recycling (% of loaded, mean±s.e.m.)	Recycling efficiency (% of control)	Velocity (μm/minute mean±s.e.m.)	Velocity (% control)
Control	79±3.1	100	0.49±0.03	100
Rab11b-GDP	29±11	35	0.78±0.08	164
Rab11a-GDP	58±1.4	73	0.76±0.04	144
Rab11b-GDP + Rab4a-N121I	72±5.5	89	0.60±0.04	123
Rab4a-N121I or Rab4a-S22N	70±4.4	88	0.54±0.05	108

respectively. As shown in Fig. 6J, this constituted, respectively, only about 9% and 12% of the control values.

To determine the origin of the wound-healing defect, we tracked the position of individual cell nuclei in a time-lapse image series taken at 4 minute intervals to analyze cell velocity and directionality of motion. Interestingly, the apparent failure of cells expressing <sup>GFP</sup>Rab11b mutants to migrate in the wound assay was not due to the inability of the cells to locomote. On the contrary, the instantaneous velocities of cells expressing <sup>GFP</sup>Rab11b mutants were at or slightly above control levels, both at the edge of the wounds and in the middle of the monolayers (Fig. 6K). However, the directionality of migration was affected. Tracks of individual control cell trajectories appeared very directional and most were oriented towards the wound (Fig. 6C). By contrast, the migration trajectories of individual cells expressing either of the GTPase defective <sup>GFP</sup>Rab11b mutants were random, including some cells moving back into the monolayer (Fig. 6F,I). Taken together, this suggests that the cells expressing mutant <sup>GFP</sup>Rab11b proteins lost their sense of directionality, and any advancement of the wound edge was a result of random cell movement, unlike in control cells, where the cells maintained contacts with each other and were moving directionally as a single front. Overall, the behavior of cells transiently or stably expressing Rab11b mutants was similar and in all cases was characterized by increased motility and decreased directionality of migration.

#### Effect of <sup>GFP</sup>Rab11b-GDP expression on cytoskeleton and adhesion proteins

In order to see whether the dramatic changes in migratory behavior correlated with reorganization of the cytoskeleton machinery in <sup>GFP</sup>Rab11b mutants, we labeled cells transiently expressing <sup>GFP</sup>Rab11b-GDP with antibodies against actin and tubulin. We found no major difference in the microtubule system between control and mutant cells (Fig. 7C), but the actin distribution was markedly affected (Fig. 7B). In control cells, actin was localized in loose bundles around the cell periphery, stress fibers across the cell body, and in a band within lamellipodia. In the <sup>GFP</sup>Rab11b-GDP mutant cells, the bundles and the stress fibers were reduced and, instead, actin-rich protrusions were observed throughout the cell periphery, even along cell-cell contacts.

To investigate whether inhibiting recycling affected cell-cell and cell-matrix adhesions, we also performed immunofluorescence to visualize the distribution of e-cadherin, a marker of cell-cell adhesions, and vinculin, a marker of focal adhesions. We did not detect significant differences in cell-cell adhesions between control cells and cells transiently expressing <sup>GFP</sup>Rab11b-GDP, either in dense monolayers, or in smaller islands (Fig. 7D-G). By contrast, focal adhesion distribution was different between control and <sup>GFP</sup>Rab11b-GDP-expressing cells. In control cells focal adhesions were

elongated in shape and concentrated at the free cell edges, corresponding to the areas of maximal lamellipodial activity. By contrast, <sup>GFP</sup>Rab11b-GDP-expressing cells had vinculin-containing focal adhesions not only at the free edges, but also in the lamellipodia protruding beneath neighboring cells in the middle of multicellular islands (Fig. 7H,I). The focal adhesions in <sup>GFP</sup>Rab11b-GDP-expressing cells also appeared shorter and more densely packed than in control cells. Thus, both actin and vinculin phenotypes correlated very well with the polarity loss and increased motility of the mutant cells.

#### Transferrin recycling efficiency inversely correlates with migration velocity

In order to investigate whether inhibiting endocytic recycling by means other than Rab11b inhibition would have a similar effect on PtK1 cell motility, we chose to overexpress in PtK1 cells the mutant forms of two other Rab proteins implicated in recycling, namely Rab11a and Rab4a. To perturb Rab11a function we microinjected the PtK1 cells with GFP-conjugated, GDP-restricted Rab11a-S25N mutant (<sup>GFP</sup>Rab11a-GDP). As expected, this induced some inhibition of transferrin recycling (58±1.4%, compared with 79±3.1% in control and 29±11% in <sup>GFP</sup>Rab11b-GDP-expressing cells, Fig. 8A, Table 1). Comparison of neighboring cells in each experiment indicated that recycling efficiency in <sup>GFP</sup>Rab11a-GDP cells was 73% of that in control cells (Fig. 8B, Table 1). This result is in agreement with previous data indicating that Rab11a may be involved in endosomal recycling (Green et al., 1997; Ren et al., 1998; Ullrich et al., 1996; Volpicelli et al., 2002). Decreased recycling in Rab11a mutants also corresponded to slightly abnormal cell shape (data not shown) and a 44% increase in cell velocity compared with that in control cells from the same coverslips (0.76 μm/minute vs. control 0.53 μm/minute, Fig. 8C, Table 1). These results confirm that decreased recycling correlates with increases in cell motility, and that this phenomenon is not limited to effects of disrupting the activity of Rab11b.

It is conceivable that inhibiting the Rab11b-dependent slow recycling pathway could cause some of the recycling material to redirect to the fast recycling pathway. To test for this possibility, we transiently expressed in PtK1 cells dominant negative mutants of Rab4a, a characterized regulator of fast endocytic recycling. We used either <sup>YFP</sup>Rab4a-N121I, a mutant unable to bind nucleotides (van der Sluijs et al., 1992), or a GDP-restricted mutant, <sup>GFP</sup>Rab4a-S22N (Roberts et al., 2001). In both cases we observed a slight decrease in recycling efficiency (88% of control values, Fig. 8B, Table 1) consistent with the notion that the majority of internalized transferrin still leaves the cells via the Rab11-dependent slow pathway. Motility of the cells expressing the Rab4a mutants was also only slightly elevated over the control levels (108% of control, Fig. 8C, Table 1). Surprisingly, when we transiently co-

expressed  $\text{GFP}^{\text{Rab11b-GDP}}$  and  $\text{YFP}^{\text{Rab4a-N121I}}$  in PtK1 cells, recycling efficiency was closer to normal than in cells expressing the Rab11b-GDP mutant alone (89% of control values, Fig. 8B, Table 1). However, again, this small effect on recycling correlated with a slight increase in cell motility (123% of control values, Fig. 8C, Table 1).

Given the variability in the degree of recycling inhibition and cell migration velocities that are observed for cells expressing different mutant proteins, we wanted to determine whether there was a relationship between these two parameters. When the data is compiled together, it becomes clear (Fig. 8D) that the slower (or more inhibited) the recycling was, the faster the cells migrated.

## Discussion

The most important finding of this report is the clear demonstration of the role of recycling in the maintenance of directionality of cell migration. In particular, we observed a remarkable correlation of the degree of transferrin recycling inhibition in epithelial PtK1 cells with the loss of polarity, while the ability to locomote remained intact or even increased. We showed that expression of Rab11b and Rab11a mutants in PtK1 cells results in decreased transferrin recycling and abnormal cellular behavior manifested by increased cell motility and disorganized protrusional activity. This surprising result does not support the original hypothesis that recycling supplies components necessary for leading edge protrusion since, if that were true, decreased, rather than increased motility would be expected in cells where recycling was inhibited.

Existing data on the relative roles of Rab11a and Rab11b in recycling from the ERC is somewhat controversial. Schlierf et al. (Schlierf et al., 2000) have shown that overexpression of Rab11b-GDP and Rab11b-GTP mutants in Vero cells strongly inhibited transferrin recycling, suggesting that GTP hydrolysis by Rab11b is essential for endosomal recycling. They also observed colocalization between Rab11b mutants and internalized transferrin. However, other authors (Lapierre et al., 2003) argued that there is interplay between Rab11a and Rab11b, possibly via competition for common effectors. They showed that in MDCK cell lines stably overexpressing Rab11b, Rab11a might be displaced from the ERC, whereas overexpression of Rab11a did not displace Rab11b. Moreover, the authors did not observe colocalization between Rab11b and transferrin in their system. This led them to conclude that Rab11b was not likely to be a major regulator of transferrin trafficking. It is

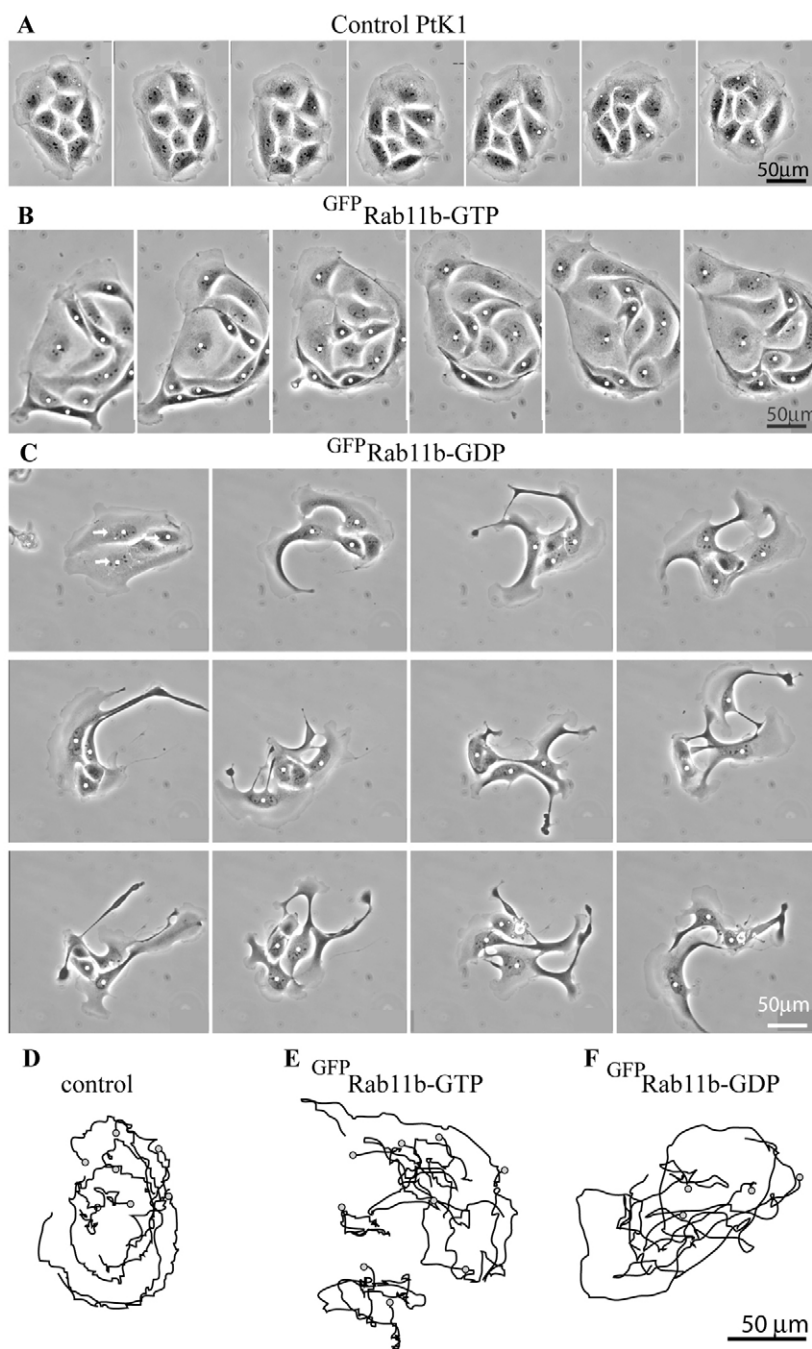


**Fig. 5.** Cells transiently expressing  $\text{GFP}^{\text{Rab11b}}$  mutants exhibit abnormal motility and morphology. The cells had been microinjected with  $\text{GFP}^{\text{Rab11b}}$  constructs approximately 4 hours before the beginning of the time-lapse, and expressing cells are marked with white dots. Frames are 40 minutes apart. (A) control PtK1 island (see also supplementary material Movie 4) and islands in which some of the cells were microinjected with either the  $\text{GFP}^{\text{Rab11b-GTP}}$  (B, supplementary material Movie 5) or  $\text{GFP}^{\text{Rab11b-GDP}}$  (C, supplementary material Movie 6) construct. The expressing cells are marked with a white dot. In C, the cells expressing high levels of  $\text{GFP}^{\text{Rab11b-GDP}}$  are marked with arrows in the first image and white dots thereafter; the unmarked cell expresses very low levels of  $\text{GFP}^{\text{Rab11b-GDP}}$ . (D-F) Tracks of migration of control cells (D) and cells expressing  $\text{GFP}^{\text{Rab11b-GTP}}$  (E) or  $\text{GFP}^{\text{Rab11b-GDP}}$  (F). Tracks were generated from 6 hour, 4-minutes interval time-lapse movies of cellular islands shown in A-C. Start positions of the cells are marked by gray circles.

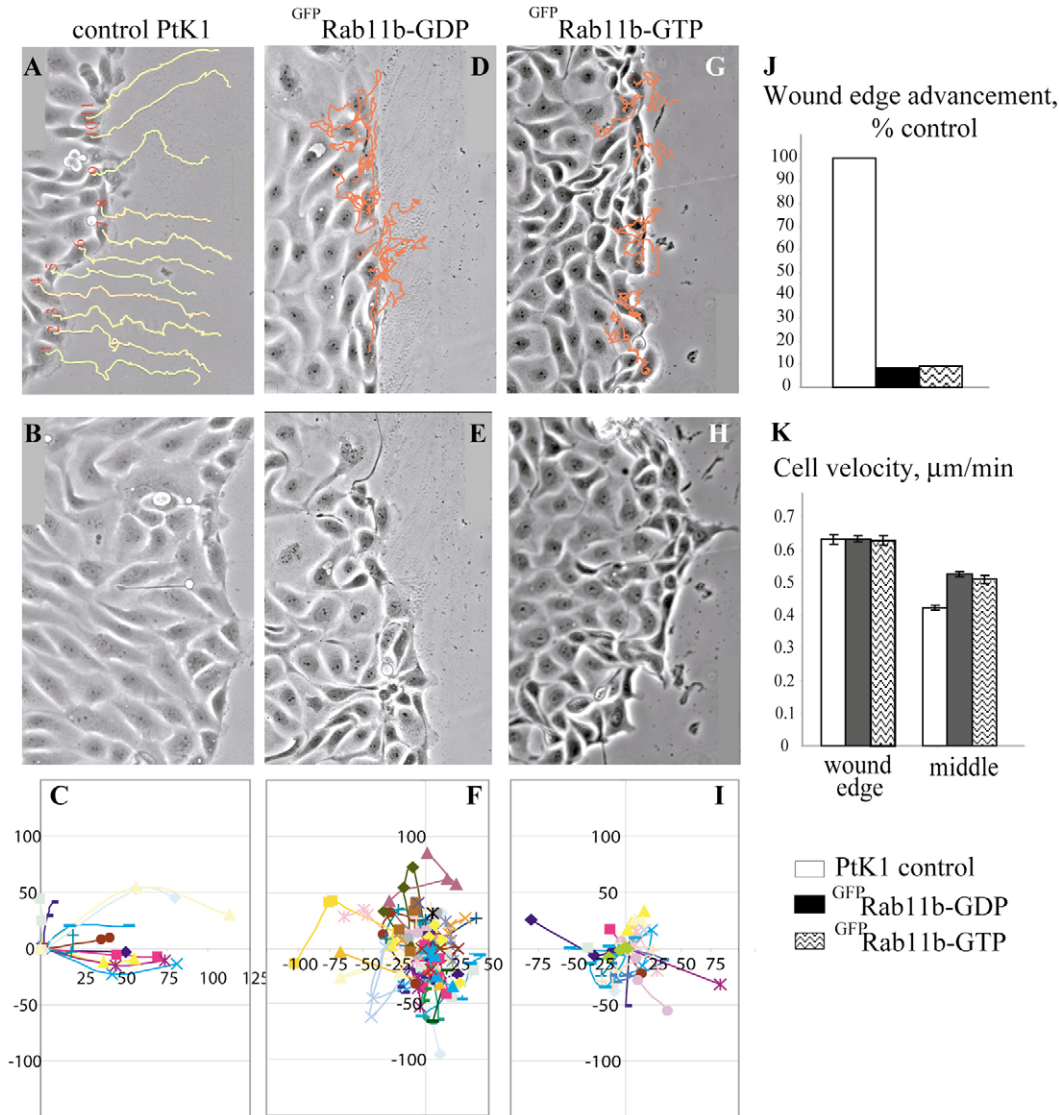


**Fig. 6.** Cells expressing  $\text{GFP}^{\text{Rab11b}}$  mutants are not able to migrate efficiently in an experimental wound assay due to a directionality defect. Confluent cell monolayers were scratch-wounded to induce migration into the wound. Positions of cells approximately 60 minutes after wounding the monolayers ('start', A,D,G,J) and 6 hours later ('finish', B,E,H,K) are shown for the control PtK1 cells (A,B), cells stably expressing  $\text{GFP}^{\text{Rab11b-GDP}}$  (D,E) and  $\text{GFP}^{\text{Rab11b-GTP}}$  (G,H). The tracks of individual cells at the wound edges, as determined from time-lapse movies, are indicated in the 'start' micrographs (A,D,G). Each frame constitutes a wound segment of approximately  $400 \mu\text{m}$  in length. Graphs in panels C, F and I show X and Y positions of individual cells at the wound edge for the mutants in the micrographs above (the starting points of all cells are placed at 0:0). Data points are 2 hours apart. (J) Average translocation of the edge (i.e. total advancement into the wound) in 6 hours. (K) Mean average velocities of the mutant Rab11b-expressing cells at the wound edges and in the middle of the monolayers. Corresponding supplemental movies are available for control (supplementary material Movie 7),  $\text{GFP}^{\text{Rab11b-GDP}}$  (supplementary material Movie 8) and  $\text{GFP}^{\text{Rab11b-GTP}}$  (supplementary material Movie 9) cells.

possible that apparent contradiction between results from these authors (Schlierf et al., 2000) may be due to their work in different systems. First of all, Schlierf et al. used transient transfections while Lapierre et al. worked on stable cell lines. Additionally, there may be intrinsic differences between cell lines.

In our experiments we observed some colocalization of  $\text{GFP}^{\text{Rab11b}}$  mutants with transferrin and a very clear inhibition of recycling in a transiently expressing system, which is in agreement with results of Schlierf et al. (Schlierf et al., 2000). When we microinjected our PtK1 cells with Rab11a or Rab11b

GDP-restricted mutants, transient (4-5 hours) expression of  $\text{GFP}^{\text{Rab11b-GDP}}$  had more influence on recycling compared with  $\text{GFP}^{\text{Rab11a-GDP}}$ . Although the absolute values of cell velocities were similar (Fig. 8C) for these two mutants, the relative increase of velocity measured as percent of the neighboring control cells (Fig. 8D, Table 1), showed a difference (144% and 164% for Rab11a-GDP and Rab11b-GDP, respectively) which correlated perfectly with the decrease in transferrin recycling (29% and 58%, respectively, Fig. 8A, Table 1).

Although we cannot exclude the possibility that, in our



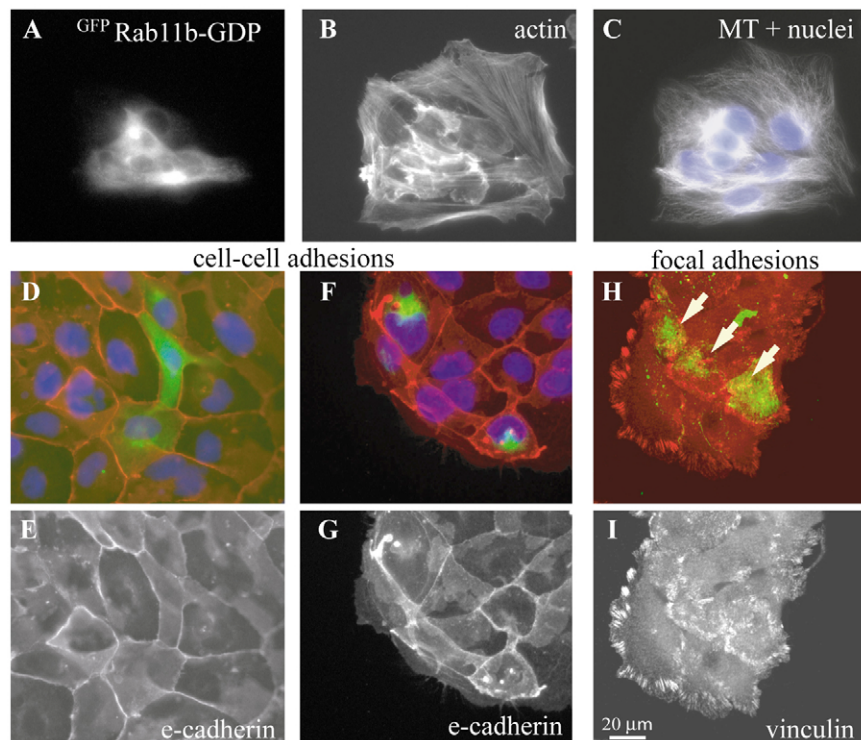


**Fig. 7.** Effects of  $GFP^{Rab11b-GDP}$  expression on the cytoskeleton and on adhesion. (A)  $GFP^{Rab11b-GDP}$ -expressing cells identified by GFP fluorescence; actin (B) and microtubules (C) identified by immunofluorescence; image of the nuclei (blue) identified by DAPI is overlaid onto the microtubule image (C). (D-G) Cell-cell adhesions visualized by indirect immunofluorescence against e-cadherin. (D,F) Pseudocolored overlay images of  $GFP^{Rab11b-GDP}$  (green), E-cadherin (red) and nuclei (blue); (E,G) E-cadherin images of the same cells. (H,I) Confocal micrographs of focal adhesions visualized by indirect immunofluorescence against vinculin. (H) Pseudocolored overlay image of  $GFP^{Rab11b-GDP}$  (green) and vinculin (red); (I) vinculin image of the same cells. Scale bar for all panels, 20  $\mu m$ .

hands, apparent effects of Rab11b were actually mediated through Rab11a, the important message is that inhibiting the slow recycling pathway leads to an increase in cell velocity and loss of polarity. Since Rab11a has been implicated in transport from the TGN (Chen et al., 1998; Chen and Wandering-Ness, 2001; Urbe et al., 1993; Wilcke et al., 2000), there is a possibility that instead of (or in addition to) the effects on recycling, the affected TGN trafficking may be responsible for the changes in cell motile behavior. We do not have direct evidence to prove or disprove this notion; however, it is probably not the case in epithelial cells since, unlike in fibroblasts, inhibition of TGN to PM transport by expression of dominant negative protein kinase D (Prigozhina and Waterman-Storer, 2004) did not have any effect on PtK1 cell motility (our unpublished data).

To our knowledge there are two other reports on the connection between Rab11-dependent recycling and cell migration (Fan et al., 2004; Mammoto et al., 1999). In the first report (Mammoto et al., 1999), the authors inhibited recycling by transiently expressing mutants of Rab11 and its downstream effector rabphilin-11 in HeLa cells and estimated cell migration by use of a gold particle uptake assay. By this method it appeared that the migration of the mutant cells was inhibited compared with the control. However, this method might not be sensitive enough since it only measured the total area covered by the migrating cells and did not take into account the fact that the cells might have been moving through the same area multiple times. It would be especially inaccurate if some of the cells were smaller in size and/or actively protruding but were unable to migrate due to polarization/directionality defects, as we observed in the present study. In the second report (Fan et al., 2004) it was shown that disruption of receptor recycling by overexpression of truncated myosin Vb and Rab11-FIP2 proteins inhibited chemotaxis but not

random migration of HEK293 cells. Our results showing that inhibition of recycling leads to non-localized protrusional activities and cell depolarization are in agreement with this data. Interestingly, variance of Rab11 expression level and, presumably, Rab11-dependent recycling has been reported to be specific in certain malignancies such as carcinoma invasion (Yoon et al., 2005) and epithelial dysplasia leading to adenocarcinoma (Goldenring et al., 1999; Werner et al., 1999), where it may contribute to loss of polarity and abnormal cell behavior.

The original hypothesis that we wanted to test was that polarized recycling from the ERC towards the leading edge is needed to supply materials and/or signals for protrusion. Since expression of Rab11 mutants that affect the slow recycling pathway through the ERC caused redistribution of the lamellipodial activity and loss of cell polarity, we hypothesized that this may be mediated via activation of fast, Rab4a-recycling. This would make sense considering that we still observed at least 29% of transferrin recycling back to the PM in cells expressing Rab11 mutants. Also, such a rerouting has been previously reported for  $\alpha v\beta 3$  integrins which, upon PDGF treatment, switch from the normal Rab11-dependent to the fast Rab4-dependent pathway (Roberts et al., 2001). Rerouting to the fast recycling pathway could make it impossible to deliver cargo preferentially to the leading edge. Instead, the endocytosed material could probably be recycled back close to the place where it was internalized, and the dynamics of the process would also be affected. To test for this possibility we looked at the effects of dominant negative mutants of Rab4a on motility of PtK1 cells. Unlike previous reports in HeLa cells (McCaffrey et al., 2001), we observed only a very small effect on recycling in PtK1 cells expressing either Rab4a-S22N or Rab4a-N121I, which correlated perfectly with a negligible (8%) increase in motility.

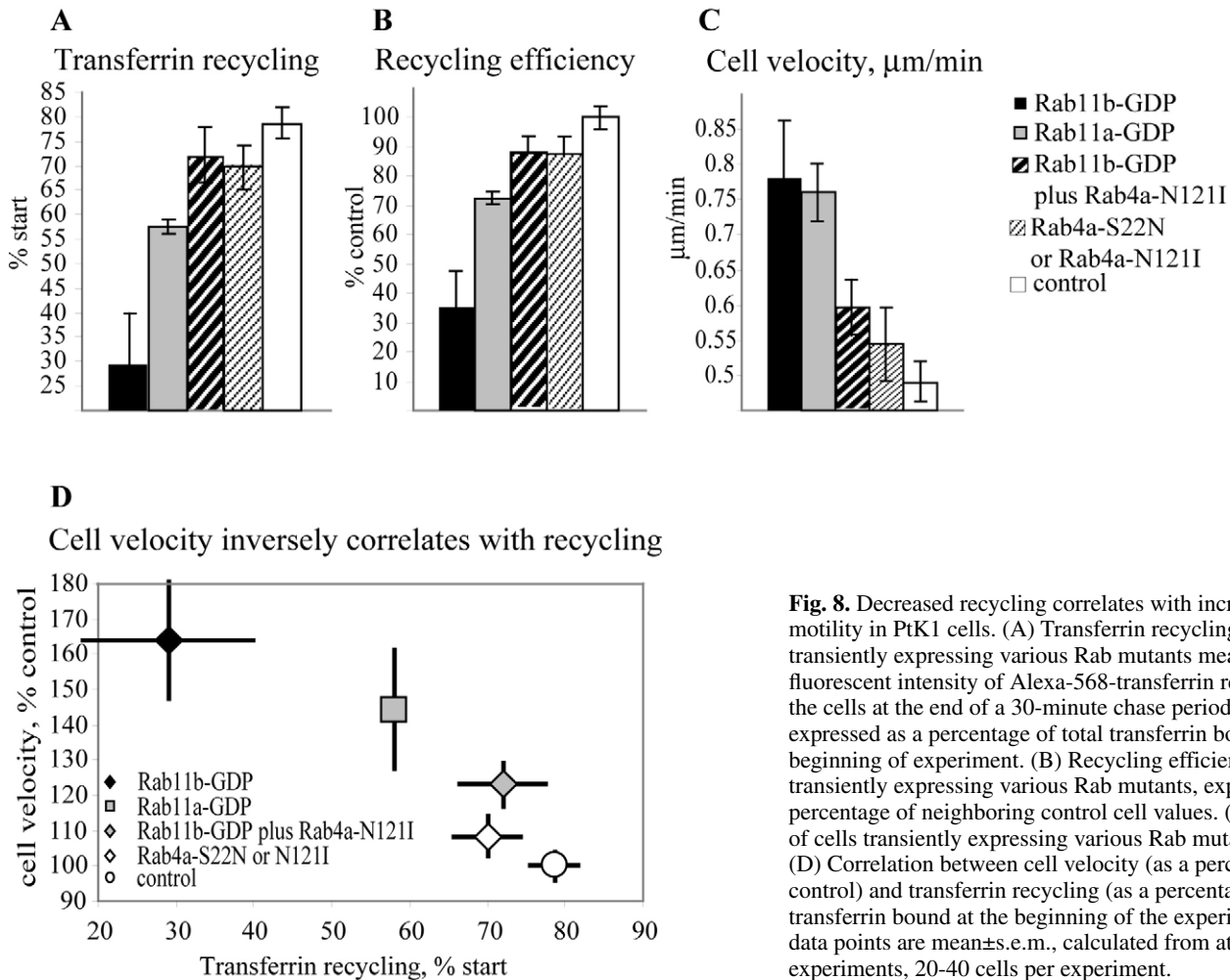


**Fig. 8.** Decreased recycling correlates with increased motility in PtK1 cells. (A) Transferrin recycling in cells transiently expressing various Rab mutants measured as fluorescent intensity of Alexa-568-transferrin retained inside the cells at the end of a 30-minute chase period, and expressed as a percentage of total transferrin bound at the beginning of experiment. (B) Recycling efficiency in cells transiently expressing various Rab mutants, expressed as a percentage of neighboring control cell values. (C) Velocities of cells transiently expressing various Rab mutants. (D) Correlation between cell velocity (as a percentage of control) and transferrin recycling (as a percentage of total transferrin bound at the beginning of the experiment). All data points are mean  $\pm$  s.e.m., calculated from at least three experiments, 20–40 cells per experiment.

Surprisingly, when we transiently co-expressed Rab11b-GDP and Rab4a-N121I in PtK1 cells, there was very little effect on transferrin recycling (89% recycling efficiency compared with the neighboring control cells) and a slight effect on cell migration (23% increase). We are not sure how to explain this result. One possibility could be that when both slow and fast recycling is inhibited, the cargo may be rerouted to some other recycling pathway and exocytosed from the cells in a non-specific manner, for example through a Rab22-dependent pathway from early endosomes (Kauppi et al., 2002; Weigert et al., 2004). Also, a potential common effector for Rab11 and Rab4 (Lindsay et al., 2002; Lindsay and McCaffrey, 2004) has been identified. In cells where both Rab11 and Rab4 are overexpressed, its interaction with the Rabs may be affected. This, in turn, might modify the overexpression phenotypes, for example, by affecting the sorting of internalized cargo (Peden et al., 2004).

The mechanism connecting recycling and motility in our experiment is likely to involve perturbation of adhesion molecule distribution and dynamics which, in turn, may modulate actin function via Rho GTPases. Our results indicate that cells expressing  $\text{GFP}^{\text{Rab11b-GDP}}$  have altered distribution of focal adhesions and actin cytoskeleton. Although, by immunofluorescence we did not observe gross defects in cell-cell adhesion organization, it is still possible that the dynamics

of these adhesions might be altered in cells expressing  $\text{GFP}^{\text{Rab11b-GDP}}$ . E-cadherin has been shown to recycle in a Rab11-dependent pathway (Lock and Stow, 2005), therefore we would expect that a more sensitive method such as fluorescent speckle microscopy, might allow detection of these differences. It is hard to prove whether the effects of recycling are mediated via actin and adhesions, or whether these changes merely reflect a less polarized and more dynamic cellular phenotype. However, it has been shown that actin remodeling during *Drosophila* embryo development requires recycling (Riggs et al., 2003) and there are reports connecting recycling, adhesions and cell motility. For example, integrins have been proposed to be internalized at the rear of the cell during tail detachment and recycled towards the front of the cells where they can participate in formation of new adhesion (Bretscher, 1996). This polarized recycling has been shown to depend on Rab11 and to affect cell motility (Powelka et al., 2004). Additional support of the proposed mechanism connecting recycling and motility comes from work of Imamura et al. (Imamura et al., 1998). The authors found that, in MDCK cells, activation of Rab5 (on early endosomes) and, to a lesser extent, of Rab11 was necessary for the reassembly of stress fibers and focal adhesions during prolonged TPA treatment. The authors also showed that Rab proteins acted upstream of RhoA, possibly through recycling of integrins. Since TPA induces

protrusions throughout cell periphery, these results are consistent with the notion that fast, non-polarized recycling from early endosomes is more important for TPA-stimulated motility than slow, Rab11b-dependent recycling from the ERC. Conversely, we hypothesize that regular motility characterized by polarized protrusions at the leading edge requires slow Rab11b-dependent, but not so much fast Rab5-dependent recycling.

It should be noted that the effect of recycling inhibition on the velocity of cell movement may differ in different cell types, possibly according to cellular adhesive properties (reviewed by Lauffenburger and Horwitz, 1996). However, we predict that delocalization of lamellipodial activity as a result of perturbed recycling from the central organelle, either ERC (this report), or the GA (Prigozhina and Waterman-Storer, 2004) may be a more universal phenomenon. In summary, contrary to our expectations, we found that in epithelial PtK1 cells decreased endosomal recycling correlates with the increased cell motility coupled to delocalization of protrusional activity. We suggest that Rab11-dependent polarized endosomal recycling is required for the regulation of cell polarity and, when disrupted, increases disorganized motility.

## Materials and Methods

### c-DNA constructs

GFP-conjugated Rab11b-wt and Rab11b-GTP (Q70L) (Schlierf et al., 2000) cDNAs in eukaryotic expression plasmids were obtained from Beate Schlierf (Institut für Biochemie, Erlangen, Germany). The Rab11b-GDP (S25N) mutant was constructed by mutagenizing Rab11b-wt using the QuickChange Mutagenesis kit (Stratagene). GFP-conjugated Rab11a cDNAs in eukaryotic expression plasmids (Hales et al., 2001; Wang et al., 2000) were obtained from James Goldenring (Vanderbilt University School of Medicine, Nashville, TN); YFP-conjugated Rab4a-N121I (<sup>YFP</sup>Rab4a-N121I) and GFP-conjugated Rab4a-S22N (<sup>GFP</sup>Rab4a-S22N) cDNAs in eukaryotic expression plasmids (Roberts et al., 2001; van der Sluijs et al., 1992) were obtained from Peter van der Sluijs (University Medical Center, Utrecht, Netherlands).

### Cell culture and microinjection

PtK1 rat kangaroo kidney epithelial cells were cultured in F12 medium supplemented with 10% fetal bovine serum (Gibco) at 37°C in a humidified atmosphere of 5% CO<sub>2</sub>. For transient expression, cDNA expression constructs (100–150 µg/ml in water) were microinjected in the cell nuclei using an Eppendorf (Hamburg, Germany) microinjection system. Cells were allowed to express GFP-fusion proteins for at least 4 hours prior to imaging. Heterogeneous cell lines stably expressing GFP-conjugated Rab11b constructs were developed by transfecting the cells using lipofectamin (Invitrogen) and growing in the presence of G418. For live-cell imaging, coverslips of cells were mounted in double-stick tape chambers, Rose chambers, or custom-made aluminum slide chambers. Typically small (4–8 cells) islands were selected for the migration experiments and small-to-medium (4–12 cells) islands were imaged in fluorescent transferrin recycle experiments. To assess the ability of cells expressing Rab11b mutants to migrate directionally, stably expressing cells were analyzed in an experimental wound assay (Kupfer et al., 1982).

### Transferrin internalization and recycling assay

For dynamic live cell imaging of transferrin internalization and transport through the endosomal system, the cells were serum-starved for at least 1 hour and then were placed on ice in serum-free media containing 50 µg/ml of Alexa-568 labeled transferrin (Molecular Probes) for 30 minutes. The cells were then rinsed, mounted in transferrin-free media and transferred to the microscope where they were warmed up to 37°C to initiate transferrin internalization. For recycling efficiency assays, cells were serum-starved for at least 1 hour and then allowed to internalize Alexa-568-labeled transferrin for 45 minutes at 37°C. The cells were then rinsed in PBS and either fixed immediately, or after a chase period of 30 minutes at 37°C in transferrin-free, serum-containing media.

### Microscopy

High resolution time-lapse live cell imaging of GFP fusion proteins and Alexa 568 transferrin was performed on the spinning disk confocal microscope system described previously (Adams et al., 2003; Salmon et al., 2002) using 60× or 100× 1.4 NA PlanApo objective lenses. Images were captured at 10 or 20 seconds

intervals. Immunofluorescent images were collected either on the confocal system described above, or on an inverted Nikon microscope utilizing epi-fluorescent illumination and equipped with electronically controlled shutters, filter wheels, and a 14-bit cooled CCD camera (Orca II, Hamamatsu Corporation) controlled by MetaMorph software (Universal Imaging Corporation). Cell motility was monitored as described (Prigozhina and Waterman-Storer, 2004) using phase contrast microscopy on an inverted microscope (Nikon TE 200) equipped with an Orca 285 CCD camera (Hamamatsu Photonics) and a robotic MS-2000 XYZ Microscope stage (Applied Scientific Instrumentation) controlled by MetaVue software (Universal Imaging/Molecular Devices). Images were collected at 4 minute intervals with a 20× 0.6 NA objective lens.

### Immunocytochemistry

Coverslips of cells were briefly rinsed in PBS (0.9% NaCl, 10 mM sodium phosphate, pH 7.2) and then fixed with either –20°C methanol for 5 minutes, or 4% paraformaldehyde for 15 minutes with subsequent permeabilization with 0.5% Triton X-100 for 5 minutes.

Golgi apparatus was visualized with TRITC-lectin (Sigma) or rabbit anti-mannosidase II antibodies (gift from Bill Balch, The Scripps Research Institute). Other antibodies used in this study were: sheep anti-TGN38 (Accurate Chemical & Scientific Corporation), mouse anti-actin (a gift from Velia Fowler, The Scripps Research Institute), rat anti-tubulin (Serotec), mouse anti-E-cadherin (BD Transduction) and mouse anti-vinculin (Sigma). All fluorescent secondary antibodies were obtained from Jackson ImmunoResearch.

### Image processing and data analysis

Micrographs were calibrated using images of a stage micrometer. All measurements were performed in MetaMorph (Universal Imaging/Molecular Devices) and the data transferred to Excel (Microsoft) for analysis and representation.

Quantification of transferrin recycling was done in two ways. First, we measured a difference in intracellular transferrin fluorescence at the beginning and at the end of the chase period (i.e. transferrin that left the cell due to recycling) and expressed it as a percentage of intracellular transferrin fluorescence at the beginning of the chase period. This number will thereafter be referred to as 'percent transferrin recycling'. Second, for each experiment we calculated the percentage of transferrin recycling in cells expressing mutant Rab and in neighboring control cells from the same coverslip and expressed the 'recycling efficiency' of the mutant cells as a percentage of the control values, taking recycling in control cells at 100%. This allowed us to normalize the data and compensate for any differences in transferring loading due to sample handling from experiment to experiment. The values from at least three experiments were then averaged and presented as mean±s.e.m.

The assay for specificity of transferrin binding was performed in a multiwell plate. PtK1 cells were incubated with four increasing concentrations (10, 50, 100 and 250 µg/ml each) of fluorescently labeled human Alexa568-transferrin and FITC-dextran either at 37°C (for 45 minutes) or on ice (for 30 minutes). Each condition was assayed in three wells, four fields of view per well, resulting in 100 cells on average per condition. Images were acquired with a 40× high NA objective on a Q3DM Eidaq robotic microscopy workstation (equivalent to a Beckman Coulter IC100). Image segmentation and analysis of cellular fluorescence was performed automatically, using Thora™ software (Vala Sciences).

Locomotory activity of cells was determined from the instantaneous velocities of the cell nucleus at 4 minute intervals. Statistical samples were formed by breaking the 4-minute interval measurements into groups of 5 (i.e. 20 minutes). The average over each group constituted one data point. The standard error of the mean is given by the standard deviation divided by the square root of the total number of 20 minute intervals. Wound edge advancement was quantified from images taken at the beginning of the time-lapse and 6 hours later by averaging the distance between the advancing wound edge and the distal edge of the field of view.

We thank Beate Schlierf (Institute for Biochemistry, Erlangen, Germany), James Goldenring (Vanderbilt University School of Medicine, Nashville, TN) and Peter van der Sluijs (University Medical Center, Utrecht, Netherlands) for providing cDNA constructs; Bill Balch (TSRI) and Velia Fowler (TSRI) for gifts of antibodies; Sandy Schmid, Hanna Damke and Defne Yarar (TSRI), as well as members of the Waterman-Storer lab, for their support and helpful discussions. This work was supported by Leukemia and Lymphoma Society Career Development grant #5195-03 to N.L.P. and by NIH GM-61804 grant to C.M.W.-S.

### References

- Adams, M. C., Salmon, W. C., Gupton, S. L., Cohan, C. S., Wittmann, T., Prigozhina, N. and Waterman-Storer, C. M. (2003). A high-speed multi-spectral spinning disk confocal microscope system for fluorescent speckle microscopy of living cells. *Methods* **1**, 29–41.

- Bergmann, J. E., Kupfer, A. and Singer, S. J. (1983). Membrane insertion at the leading edge of motile fibroblasts. *Proc. Natl. Acad. Sci. USA* **80**, 1367-1371.
- Bretscher, M. S. (1984). Endocytosis: relation to capping and cell locomotion. *Science* **224**, 681-686.
- Bretscher, M. S. (1992). Cells can use their transferrin receptors for locomotion. *EMBO J.* **11**, 383-389.
- Bretscher, M. S. (1996). Moving membrane up to the front of migrating cells. *Cell* **85**, 465-467.
- Bretscher, M. S. and Aguado-Velasco, C. (1998a). EGF induces recycling membrane to form ruffles. *Curr. Biol.* **8**, 721-724.
- Bretscher, M. S. and Aguado-Velasco, C. (1998b). Membrane traffic during cell locomotion. *Curr. Opin. Cell Biol.* **10**, 537-541.
- Bucci, C., Parton, R. G., Mather, I. H., Stunnenberg, H., Simons, K., Hoflack, B. and Zerial, M. (1992). The small GTPase rab5 functions as a regulatory factor in the early endocytic pathway. *Cell* **70**, 715-728.
- Chavrier, P., van der Sluijs, P., Mishal, Z., Nagelkerken, B. and Gorvel, J. P. (1997). Early endosome membrane dynamics characterized by flow cytometry. *Cytometry* **29**, 41-49.
- Chen, W. and Wandinger-Ness, A. (2001). Expression and functional analyses of Rab8 and Rab11a in exocytic transport from trans-Golgi network. *Methods Enzymol.* **329**, 165-175.
- Chen, W., Feng, Y., Chen, D. and Wandinger-Ness, A. (1998). Rab11 is required for trans-golgi network-to-plasma membrane transport and a preferential target for GDP dissociation inhibitor. *Mol. Biol. Cell* **9**, 3241-3257.
- Daro, E., van der Sluijs, P., Galli, T. and Mellman, I. (1996). Rab4 and cellubrevin define different early endosome populations on the pathway of transferrin receptor recycling. *Proc. Natl. Acad. Sci. USA* **93**, 9559-9564.
- Fan, G. H., Lapierre, L. A., Goldenring, J. R., Sai, J. and Richmond, A. (2004). Rab11-family interacting protein 2 and myosin Vb are required for CXCR2 recycling and receptor-mediated chemotaxis. *Mol. Biol. Cell* **15**, 2456-2469.
- Goldenring, J. R., Smith, J., Vaughan, H. D., Cameron, P., Hawkins, W. and Navarre, J. (1996). Rab11 is an apically located small GTP-binding protein in epithelial tissues. *Am. J. Physiol.* **270**, G515-G525.
- Goldenring, J. R., Ray, G. S. and Lee, J. R. (1999). Rab11 in dysplasia of Barrett's epithelia. *Yale J. Biol. Med.* **72**, 113-120.
- Green, E. G., Ramm, E., Riley, N. M., Spiro, D. J., Goldenring, J. R. and Wessling-Resnick, M. (1997). Rab11 is associated with transferrin-containing recycling compartments in K562 cells. *Biochem. Biophys. Res. Commun.* **239**, 612-616.
- Hales, C. M., Griner, R., Hobdy-Henderson, K. C., Dorn, M. C., Hardy, D., Kumar, R., Navarre, J., Chan, E. K., Lapierre, L. A. and Goldenring, J. R. (2001). Identification and characterization of a family of Rab11-interacting proteins. *J. Biol. Chem.* **276**, 39067-39075.
- Heath, J. P. and Holfield, B. F. (1991). Cell locomotion: new research tests old ideas on membrane and cytoskeletal flow. *Cell Motil. Cytoskeleton* **18**, 245-257.
- Hopkins, C. R., Gibson, A., Shipman, M., Strickland, D. K. and Trowbridge, I. S. (1994). In migrating fibroblasts, recycling receptors are concentrated in narrow tubules in the pericentriolar area, and then routed to the plasma membrane of the leading lamella. *J. Cell Biol.* **125**, 1265-1274.
- Imamura, H., Takaishi, K., Nakano, K., Kodama, A., Oishi, H., Shiozaki, H., Monden, M., Sasaki, T. and Takai, Y. (1998). Rho and Rab small G proteins coordinately reorganize stress fibers and focal adhesions in MDCK cells. *Mol. Biol. Cell* **9**, 2561-2575.
- Kauppi, M., Simonsen, A., Bremnes, B., Vieira, A., Callaghan, J., Stenmark, H. and Olkkonen, V. M. (2002). The small GTPase Rab22 interacts with EEA1 and controls endosomal membrane trafficking. *J. Cell Sci.* **115**, 899-911.
- Kupfer, A., Louvard, D. and Singer, S. J. (1982). Polarization of the Golgi apparatus and the microtubule-organizing center in cultured fibroblasts at the edge of an experimental wound. *Proc. Natl. Acad. Sci. USA* **79**, 2603-2607.
- Lai, F., Stubbs, L. and Artzt, K. (1994). Molecular analysis of mouse Rab11b: a new type of mammalian YPT/Rab protein. *Genomics* **22**, 610-616.
- Lapierre, L. A., Dorn, M. C., Zimmerman, C. F., Navarre, J., Burnette, J. O. and Goldenring, J. R. (2003). Rab11b resides in a vesicular compartment distinct from Rab11a in parietal cells and other epithelial cells. *Exp. Cell Res.* **290**, 322-331.
- Lauffenburger, D. A. and Horwitz, A. F. (1996). Cell migration: a physically integrated molecular process. *Cell* **84**, 359-369.
- Lindsay, A. J. and McCaffrey, M. W. (2004). Characterisation of the Rab binding properties of Rab coupling protein (RCP) by site-directed mutagenesis. *FEBS Lett.* **571**, 86-92.
- Lindsay, A. J., Hendrick, A. G., Cantalupo, G., Senic-Matuglia, F., Goud, B., Bucci, C. and McCaffrey, M. W. (2002). Rab coupling protein (RCP), a novel Rab4 and Rab11 effector protein. *J. Biol. Chem.* **277**, 12190-12199.
- Lock, J. G. and Stow, J. L. (2005). Rab11 in recycling endosomes regulates the sorting and basolateral transport of E-cadherin. *Mol. Biol. Cell* **16**, 1744-1755.
- Mammoto, A., Ohtsuka, T., Hotta, I., Sasaki, T. and Takai, Y. (1999). Rab11BP/Rabphilin-11, a downstream target of rab11 small G protein implicated in vesicle recycling. *J. Biol. Chem.* **274**, 25517-25524.
- Maxfield, F. R. and McGraw, T. E. (2004). Endocytic recycling. *Nat. Rev. Mol. Cell Biol.* **5**, 121-132.
- McCaffrey, M. W., Bielli, A., Cantalupo, G., Mora, S., Roberti, V., Santillo, M., Drummond, F. and Bucci, C. (2001). Rab4 affects both recycling and degradative endosomal trafficking. *FEBS Lett.* **495**, 21-30.
- Mitchison, T. J. and Cramer, L. P. (1996). Actin-based cell motility and cell locomotion. *Cell* **84**, 371-379.
- Mohrmann, K. and van der Sluijs, P. (1999). Regulation of membrane transport through the endocytic pathway by rabGTPases. *Mol. Membr. Biol.* **16**, 81-87.
- Mohrmann, K., Gerez, L., Oorschot, V., Klumperman, J. and van der Sluijs, P. (2002). Rab4 function in membrane recycling from early endosomes depends on a membrane to cytoplasm cycle. *J. Biol. Chem.* **277**, 32029-32035.
- Mukherjee, S., Ghosh, R. N. and Maxfield, F. R. (1997). Endocytosis. *Physiol. Rev.* **77**, 759-803.
- Peden, A. A., Schonteich, E., Chun, J., Junutula, J. R., Scheller, R. H. and Prekeris, R. (2004). The RCP-Rab11 complex regulates endocytic protein sorting. *Mol. Biol. Cell* **15**, 3530-3541.
- Pierini, L. M., Lawson, M. A., Eddy, R. J., Hendey, B. and Maxfield, F. R. (2000). Oriented endocytic recycling of alpha5beta1 in motile neutrophils. *Blood* **95**, 2471-2480.
- Powelka, A. M., Sun, J., Li, J., Gao, M., Shaw, L. M., Sonnenberg, A. and Hsu, V. W. (2004). Stimulation-dependent recycling of integrin beta1 regulated by ARF6 and Rab11. *Traffic* **5**, 20-36.
- Prigozhina, N. L. and Waterman-Storer, C. M. (2004). Protein kinase D-mediated anterograde membrane trafficking is required for fibroblast motility. *Curr. Biol.* **14**, 88-98.
- Ren, M., Xu, G., Zeng, J., De Lemos-Chiarandini, C., Adesnik, M. and Sabatini, D. D. (1998). Hydrolysis of GTP on rab11 is required for the direct delivery of transferrin from the pericentriolar recycling compartment to the cell surface but not from sorting endosomes. *Proc. Natl. Acad. Sci. USA* **95**, 6187-6192.
- Riggs, B., Rothwell, W., Mische, S., Hickson, G. R., Matheson, J., Hays, T. S., Gould, G. W. and Sullivan, W. (2003). Actin cytoskeleton remodeling during early Drosophila furrow formation requires recycling endosomal components Nuclear-fallout and Rab11. *J. Cell Biol.* **163**, 143-154.
- Ridley, A. J., Schwartz, M. A., Burridge, K., Firtel, R. A., Ginsberg, M. H., Borisy, G., Parsons, J. T. and Horwitz, A. R. (2003). Cell migration: integrating signals from front to back. *Science* **302**, 1704-1709.
- Roberts, M., Barry, S., Woods, A., van der Sluijs, P. and Norman, J. (2001). PDGF-regulated rab4-dependent recycling of alphavbeta3 integrin from early endosomes is necessary for cell adhesion and spreading. *Curr. Biol.* **11**, 1392-1402.
- Rodman, J. S. and Wandinger-Ness, A. (2000). Rab GTPases coordinate endocytosis. *J. Cell Sci.* **113**, 183-192.
- Sabe, H. (2003). Requirement for Arf6 in cell adhesion, migration, and cancer cell invasion. *J. Biochem.* **134**, 485-489.
- Salmon, W. C., Adams, M. C. and Waterman-Storer, C. M. (2002). Dual-wavelength fluorescent speckle microscopy reveals coupling of microtubule and actin movements in migrating cells. *J. Cell Biol.* **158**, 31-37.
- Schlierf, B., Fey, G. H., Hauber, J., Hocke, G. M. and Rosorius, O. (2000). Rab11b is essential for recycling of transferrin to the plasma membrane. *Exp. Cell Res.* **259**, 257-265.
- Sonnichsen, B., de Renzis, S., Nielsen, E., Rietdorf, J. and Zerial, M. (2000). Distinct membrane domains on endosomes in the recycling pathway visualized by multicolor imaging of Rab4, Rab5, and Rab11. *J. Cell Biol.* **149**, 901-914.
- Spaargaren, M. and Bos, J. L. (1999). Rab5 induces Rac-independent lamellipodia formation and cell migration. *Mol. Biol. Cell* **10**, 3239-3250.
- Trischler, M., Stoorvogel, W. and Ullrich, O. (1999). Biochemical analysis of distinct Rab5- and Rab11-positive endosomes along the transferrin pathway. *J. Cell Sci.* **112**, 4773-4783.
- Ullrich, O., Reinsch, S., Urbe, S., Zerial, M. and Parton, R. G. (1996). Rab11 regulates recycling through the pericentriolar recycling endosome. *J. Cell Biol.* **135**, 913-924.
- Urbe, S., Huber, L. A., Zerial, M., Tooze, S. A. and Parton, R. G. (1993). Rab11, a small GTPase associated with both constitutive and regulated secretory pathways in PC12 cells. *FEBS Lett.* **334**, 175-182.
- van der Sluijs, P., Hull, M., Webster, P., Male, P., Goud, B. and Mellman, I. (1992). The small GTP-binding protein rab4 controls an early sorting event on the endocytic pathway. *Cell* **70**, 729-740.
- Volpicelli, L. A., Lah, J. J., Fang, G., Goldenring, J. R. and Levey, A. I. (2002). Rab11a and myosin Vb regulate recycling of the M4 muscarinic acetylcholine receptor. *J. Neurosci.* **22**, 9776-9784.
- Wang, X., Kumar, R., Navarre, J., Casanova, J. E. and Goldenring, J. R. (2000). Regulation of vesicle trafficking in madin-darby canine kidney cells by Rab11a and Rab25. *J. Biol. Chem.* **275**, 29138-29146.
- Weigert, R., Yeung, A. C., Li, J. and Donaldson, J. G. (2004). Rab22a regulates the recycling of membrane proteins internalized independently of clathrin. *Mol. Biol. Cell* **15**, 3758-3770.
- Werner, M., Mueller, J., Walch, A. and Hofer, H. (1999). The molecular pathology of Barrett's esophagus. *Histol. Histopathol.* **14**, 553-559.
- Wilcke, M., Johannes, L., Galli, T., Mayau, V., Goud, B. and Salamero, J. (2000). Rab11 regulates the compartmentalization of early endosomes required for efficient transport from early endosomes to the trans-golgi network. *J. Cell Biol.* **151**, 1207-1220.
- Yamashiro, D. J., Tycko, B., Fluss, S. R. and Maxfield, F. R. (1984). Segregation of transferrin to a mildly acidic (pH 6.5) para-Golgi compartment in the recycling pathway. *Cell* **37**, 789-800.
- Yoon, S. O., Shin, S. and Mercurio, A. M. (2005). Hypoxia stimulates carcinoma invasion by stabilizing microtubules and promoting the Rab11 trafficking of the alpha6beta4 integrin. *Cancer Res.* **65**, 2761-2769.
- Zerial, M. and McBride, H. (2001). Rab proteins as membrane organizers. *Nat. Rev. Mol. Cell Biol.* **2**, 107-117.